Areal shot record technology: Macro model estimation

Walter Rietveld[1]
Jan Thorbecke[2]

10.1 Introduction

For prestack migration it is essential to have a description of the propagation properties of the subsurface. A macro model describes these propagation properties. In DELPHI Volume IV, Chapter 10 (1993), a new approach to macro model estimation was discussed, based on the double illumination principle that we introduced in DELPHI Volume III, Chapter 5 (1992). It was shown that with the double illumination it is possible to update both *local* macro velocities and depth values as well as validate an *entire* macro boundary, 2-D or 3-D. The relation between the synthesis operator and the areal shot record was shown for the two types of illumination assuming a correct macro model. This relationship was illustrated with a simple synthetic example and on field data. Also a brief discussion on the influence of errors in the macro model was given.

In this Chapter we will review briefly the relation between the areal shot record and the synthesis operator, i.e. the basis of this new method. Next we will show how different illuminating wavefields can encounter different errors in the macro model. Especially the discrimination between velocity and depth errors, and the determination of the lateral extension of a macro boundary require two totally different illuminating wavefields. Updating algorithms for both

1. E-mail: walter@delphi.tn.tudelft.nl
2. E-mail: jan@delphi.tn.tudelft.nl

cases will be discussed together with some simple examples. Finally conclusions will be drawn and future plans will be presented.

10.2 Relation between the synthesis operator and the areal shot record

In DELPHI Volume IV, Chapter 10 (1993), a detailed discussion was given on the relation between the synthesis operator and the areal shot record. A brief review will be given in this section.

First we recall the forward model for the one-reflector case:

$$\boldsymbol{P}^{-}(z_0) = \boldsymbol{W}^{-}(z_0,z_m)\ \boldsymbol{R}^{+}(z_m)\ \boldsymbol{W}^{+}(z_m,z_0)\ \boldsymbol{S}^{+}(z_0), \tag{10.1}$$

in which $\boldsymbol{S}^{+}(z_0)$ represents the source matrix, $\boldsymbol{W}^{+}(z_m,z_0)$ the downward propagation from the surface z_0 to the reflector z_m, $\boldsymbol{R}^{+}(z_m)$ the reflectivity matrix, describing the angle dependent reflectivity for all points along the reflector, $\boldsymbol{W}^{-}(z_0,z_m)$ the upward propagation from the reflector z_m to the surface z_0, and $\boldsymbol{P}^{-}(z_0)$ the monochromatic data matrix. Note that we may have $z_m = z_m(x,y)$.

If we assume that the data is corrected for directivity, source matrix $\boldsymbol{S}^{+}(z_0)$ simplifies to:

$$\boldsymbol{S}^{+}(z_0) = \boldsymbol{I}\ S(\omega), \tag{10.2}$$

with $\boldsymbol{I}$ the identity matrix and $S(\omega)$ the source signature.

The relation between a desired illuminating wavefield $\vec{S}^{+}_{syn}(z_m)$ and the source wavefield at the surface $\vec{S}^{+}_{syn}(z_0)$ is given by:

$$\vec{S}^{+}_{syn}(z_0) = [\boldsymbol{W}^{+}(z_m,z_0)]^{-1}\ \vec{S}^{+}_{syn}(z_m), \tag{10.3a}$$

or for the synthesis operators:

$$\vec{\Gamma}^{+}(z_0) = [\boldsymbol{W}^{+}(z_m,z_0)]^{-1}\ \vec{\Gamma}^{+}(z_m), \tag{10.3b}$$

where the relation between the illuminating wavefield and the synthesis operators is given by:

$$\vec{S}^{+}_{syn}(z_0) = \vec{\Gamma}^{+}(z_0)\ S(\omega), \tag{10.3c}$$

and

$$\vec{S}^{+}_{syn}(z_m) = \vec{\Gamma}^{+}(z_m)\ S(\omega). \tag{10.3d}$$

Application of the synthesis operator $\vec{\Gamma}^{+}(z_0)$ at the surface to the data $\boldsymbol{P}^{-}(z_0)$ leaves the areal shot record $\vec{P}^{-}_{syn}(z_0)$:

$$\vec{P}^{-}_{syn}(z_0) = \boldsymbol{W}^{-}(z_0,z_m)\, \boldsymbol{R}^{+}(z_m)\, \vec{\Gamma}^{+}(z_m)\, S(\omega), \tag{10.4a}$$

or neglecting the source signature term for notation convenience:

$$\vec{P}^{-}_{syn}(z_0) = \boldsymbol{P}^{-}(z_0)\, \vec{\Gamma}^{+}(z_0) = \boldsymbol{W}^{-}(z_0,z_m)\, \vec{R}^{+}(z_m), \tag{10.4b}$$

in which,

$$\vec{R}^{+}(z_m) = \boldsymbol{R}^{+}(z_m)\, \vec{\Gamma}^{+}(z_m). \tag{10.4c}$$

Recalling that for the inverse of the downward propagation operator $\boldsymbol{W}^{+}(z_m,z_0)$ usually the match filter approach is used, i.e.:

$$[\boldsymbol{W}^{+}(z_m,z_0)]^{-1} = [\boldsymbol{W}^{-}(z_0,z_m)]^{*}, \tag{10.5}$$

in which * denotes that the complex conjugate should be taken, we can rewrite equation (10.3b) to:

$$\vec{\Gamma}^{+}(z_0) = [\boldsymbol{W}^{-}(z_0,z_m)]^{*}\, \vec{\Gamma}^{+}(z_m). \tag{10.6}$$

From equations (10.6), (10.4b) and (10.4c) we see that:

$$\vec{P}^{-}_{syn}(z_0) = [\vec{\Gamma}^{+}(z_0)]^{*}, \tag{10.7a}$$

if

$$\vec{\Gamma}^{+}(z_m) = [\vec{R}^{+}(z_m)]^{*}. \tag{10.7b}$$

The areal shot record $\vec{P}^{-}_{syn}(z_0)$ can be seen as the *half-way* response at the surface z_0 due to a source wavefield $\vec{\Gamma}^{+}(z_m)$ at z_m. The propagation properties at the source side have been corrected for via the synthesis operator $\vec{\Gamma}^{+}(z_0)$, using the defined macro model. At the receiver side the propagation properties are described by the *data*. The synthesis operator $\vec{\Gamma}^{+}(z_0)$ describes the propagation properties from the reflector at z_m to the surface z_0 entirely described by the *macro model*. A comparison of both gathers gives an indication if the propagation properties are well described by the macro model. An example will be given for two types of illumination. The model as shown in Figure 10.1 is used for the example.

The first type of illumination we will show is the *focus point* illumination:

$$\vec{\Gamma}^{+}(z_m) = \vec{\Gamma}^{+}_{i,\,m}(z_m) = \vec{I}_i(z_m) = [0, \ldots ,0,1,0, \ldots ,0]^{T}, \tag{10.8a}$$

where the indeces i and m represents the lateral position i at which the focussing point is positioned at z_m. Substitution of equation (10.8a) in equation (10.4b) and (10.6) leaves:

$$\vec{P}^{-}_{syn}(z_0) = \boldsymbol{R}_{dia}(z_0)\, [\vec{\Gamma}^{+}_{i,\,m}(z_0)]^{*}, \tag{10.8b}$$

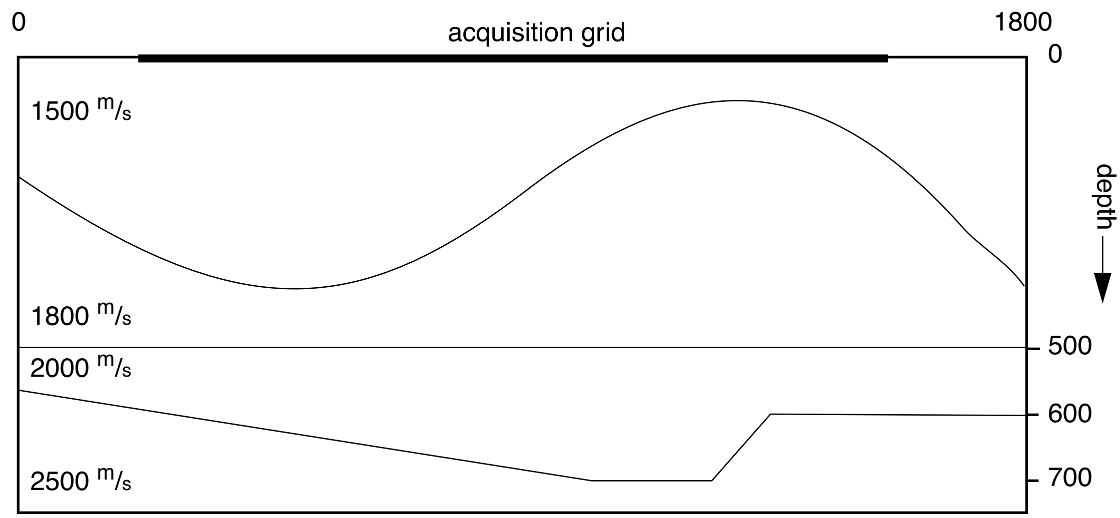

Figure 10.1: *Model used for the example. Fixed spread data was acquired within the indicated region. 128 shots were modelled, with a spacing of 12m.*

where $\boldsymbol{R}_{dia}(z_0)$ represents a diagonal matrix, describing the AVO effects at the surface z_0 due to the angle-dependent reflectivity properties at the focus point at z_m. Hence the broad band versions of $\vec{P}^{-}_{syn}(z_0)$ and $[\vec{\Gamma}^{+}_{i,\,m}(z_0)]^{*}$ are equal in traveltime, but may differ in amplitude due to these angle-dependent reflection coefficient at i. Figure 10.2 shows the time responses of the complex conjugate of the synthesis operator and the areal shot record. Note the good match

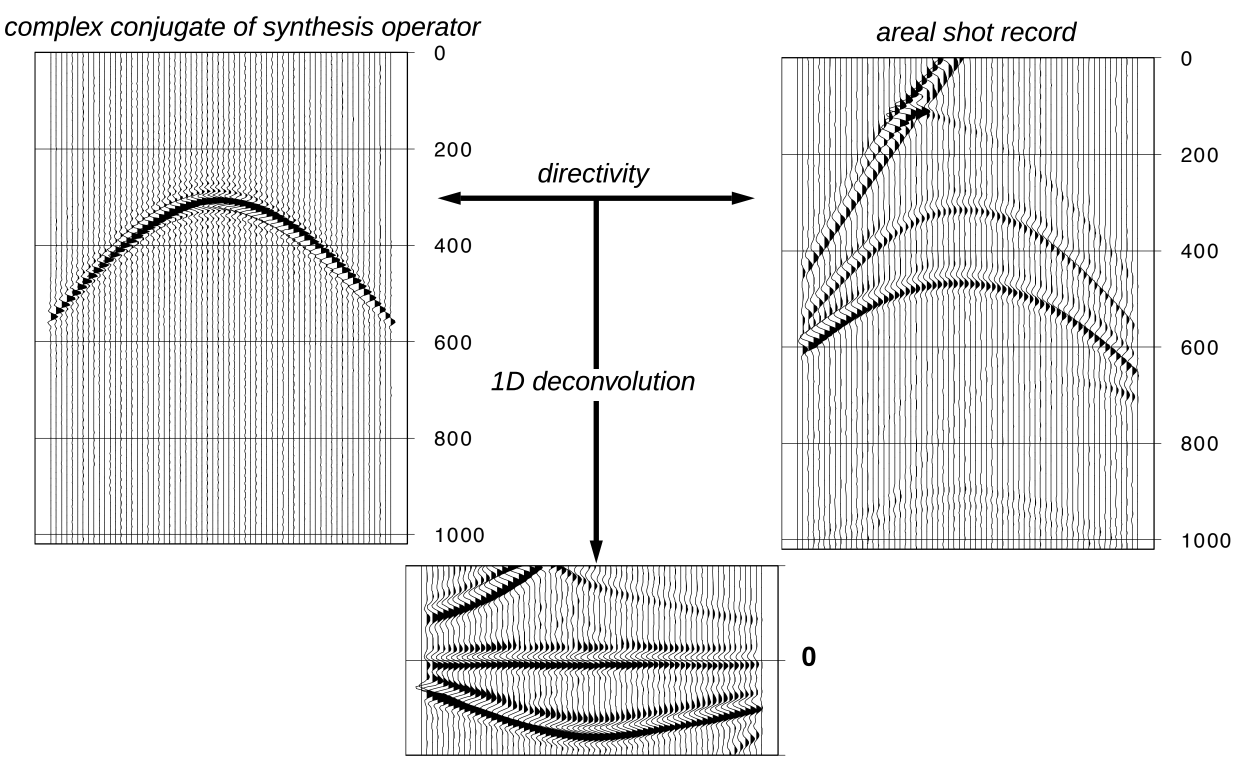

Figure 10.2: *The complex conjugate of the synthesis operator for a* focus point *illumination of the second boundary (left), and its areal shot record (right). Note that in the deconvolution display the event at* t=0 *aligns perfectly, indicating that the model is correct.*

between the event in the synthesis operator and the corresponding event in the areal shot record. In Figure 10.2 also the deconvolution of the areal shot record with the synthesis operator is shown. Note that $R(z_0)$ is in this case laterally varying and describes the angle dependent behaviour of the reflection.

The second type of illumination we will show is the *normal incidence* illumination:

$$\vec{\Gamma}^{+}(z_m) = \vec{\Gamma}^{+}_{0}(z_m) = [1,1, \ldots ,1]^T, \tag{10.9a}$$

where the index 0 indicates that the illumination angle is 0°. Substitution of equation (10.9a) in equation (10.4b) and (10.6) leaves:

$$\vec{P}^{-}_{syn}(z_0) = r_0\,[\vec{\Gamma}^{+}_{0}(z_0)]^{*}, \tag{10.9b}$$

where r_0 is the normal incidence reflection coefficient of the illuminated boundary. Figure 10.3 shows the time responses of the complex conjugate of the synthesis operator and the areal shot record. Note the good match between the event in the synthesis operator and the corresponding event in the areal shot record.

Using the relations given by equation (10.4b) and (10.6), it was shown in DELPHI Volume IV, Chapter 10 (1993) that we can evaluate macro boundaries, using different types of illuminating wavefields. This was shown both on synthetic (Figure 10.2 and 10.3) and on a field data example.

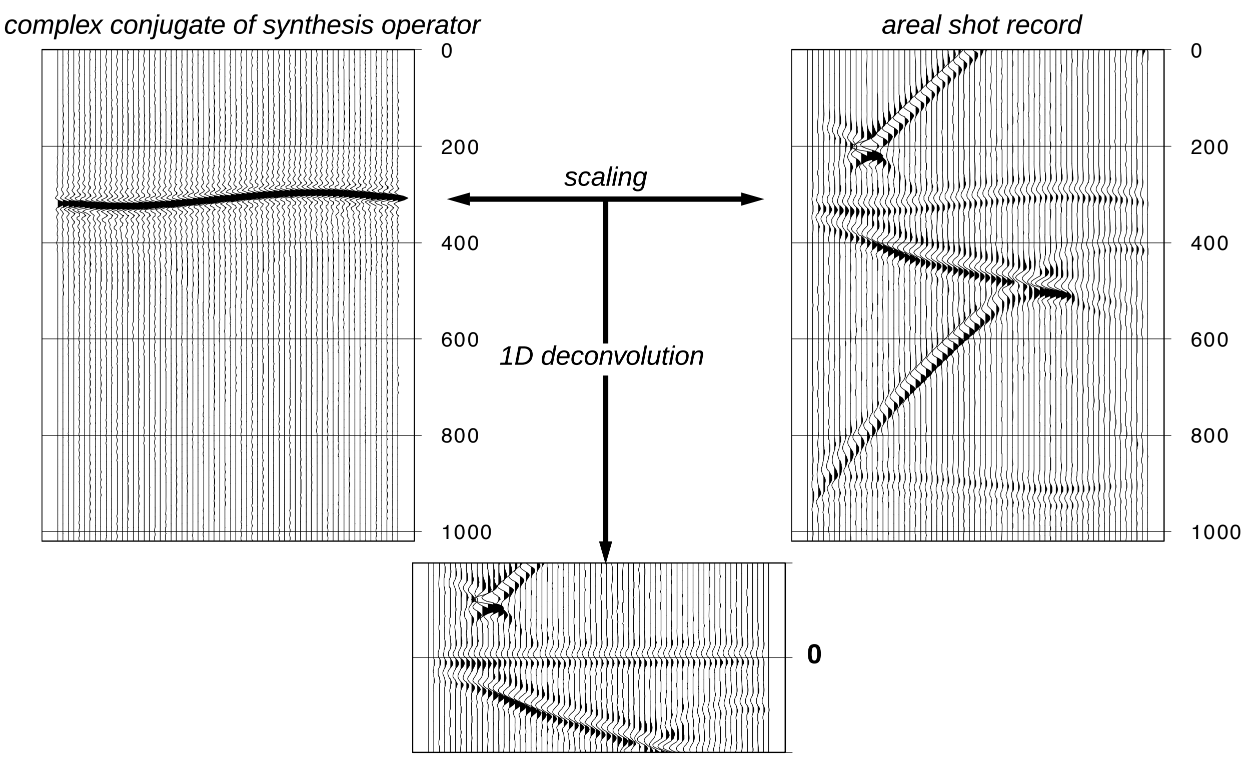

Figure 10.3: *The complex conjugate of the synthesis operator for a* normal incidence *illumination of the second boundary of the model (left), and its areal shot record (right). Note that in the deconvolution display the event at* t=0 *aligns perfectly.*

10.3 Discrimination between structural errors and depth/velocity errors

In the previous section the relation between the synthesis operator and the areal shot record have been shown briefly. Two examples for two different illuminating wavefields showed that this relation can be used to evaluate a macro boundary. In this section we will show that different type of illumination need to be used to be able to update a macro model in a lateral, i.e. structural, sense and in a depth, i.e. velocity/depth, sense. We will show that using the focus point illumination the ambiguity of a velocity and depth error can be overcome, and that the normal incidence illumination can be used to evaluate the lateral extension and structure of a macro boundary. The aim of this section is merely to show that different illuminating wavefields can detect different types of errors. The actual correction of the model, the updating will be discussed in the next section.

10.3.1 Combined velocity/depth errors

Consider again the model as shown in Figure 10.1. In the following examples we will introduce errors in this model and look how these errors appear in the synthesis operator and the areal shot record. We will focus on the second boundary. First we will change the velocity below the first layer to 1600 $^{m}/_{s}$. Simultaneously we also change the definition of the second boundary in such a way that the *one-way* traveltime of a normal incidence ray at the second boundary is approximately equal for the true model and the erroneous model. In fact we correct the *velocity* error

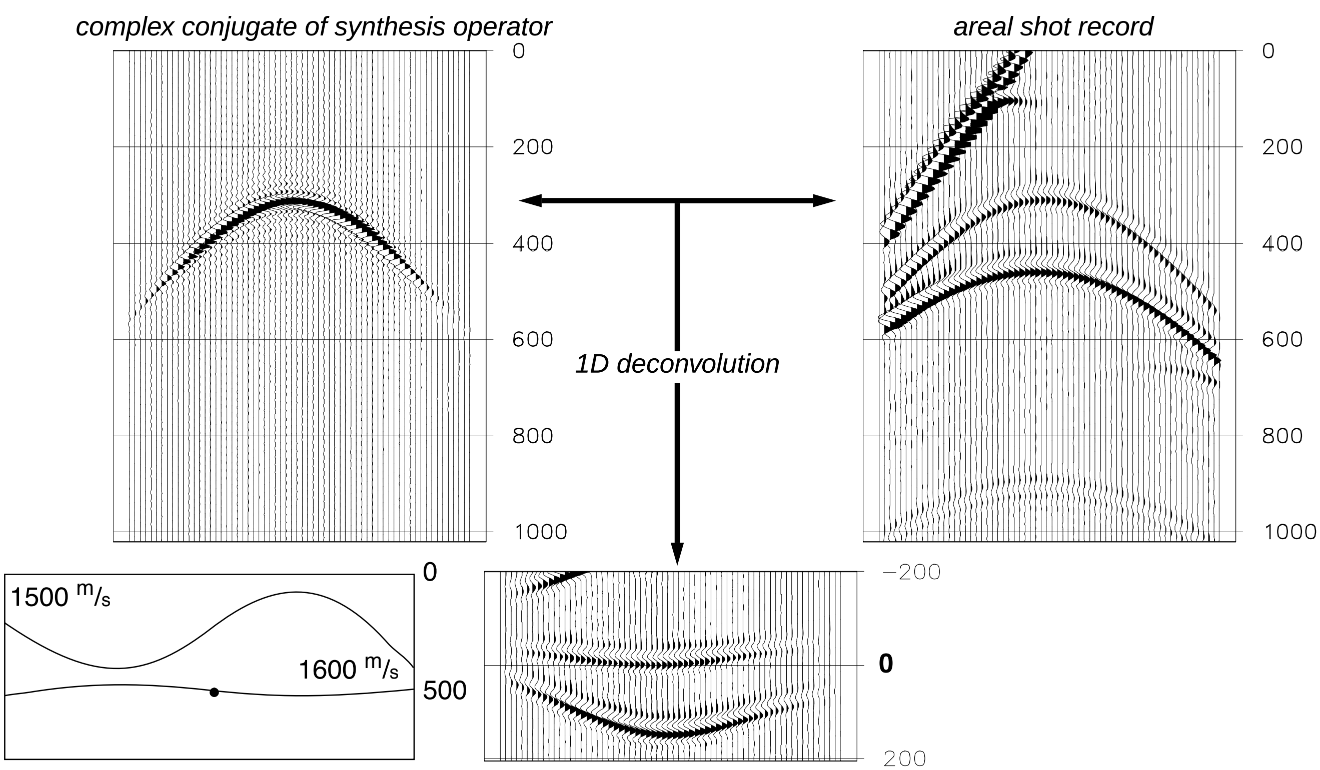

Figure 10.4: *The complex conjugate of the synthesis operator for a* focus point *illumination of the second boundary of the model (left), and its areal shot record (right). Note that in the deconvolution display the event does not align at* t=0, *indicating an error in the macro model.*

by an error in the depth of the reflector. First we will look at the result after focus point illumination. Figure 10.4 shows the time responses of the complex conjugate of the synthesis operator and the areal shot record. Note that in the deconvolution result the event does not align at $t = 0$ anymore, indicating an error in the macro model. Hence with a *focus point* illumination we can detect the introduced combined velocity/depth error.

We will now look at the result for the normal incidence illumination of the (erroneous) macro boundary. Figure 10.5 shows the time responses of the complex conjugate of the synthesis operator and the areal shot record. Note that in the deconvolution result the event *does* align at $t = 0$, although the used macro model was erroneous. Hence with a *normal incidence* illumination we cannot detect the introduced combined velocity/depth error. More general, to overcome the ambiguity between a combined velocity/depth error, the macro boundary should be illuminated by more than *one* angle. With the *focus point* illumination, that is exactly the case. The only drawback of this illumination is, that it works *locally.*

10.3.2 Structural errors

In the next example we will again consider the second macro layer, and its boundary. We take the correct velocity (1800 $^{m}/_{s}$), but reshape the structure of the boundary. At the position of the focus point the boundary is horizontal and at the correct depth of 500m. At other positions the boundary is positioned too deep.

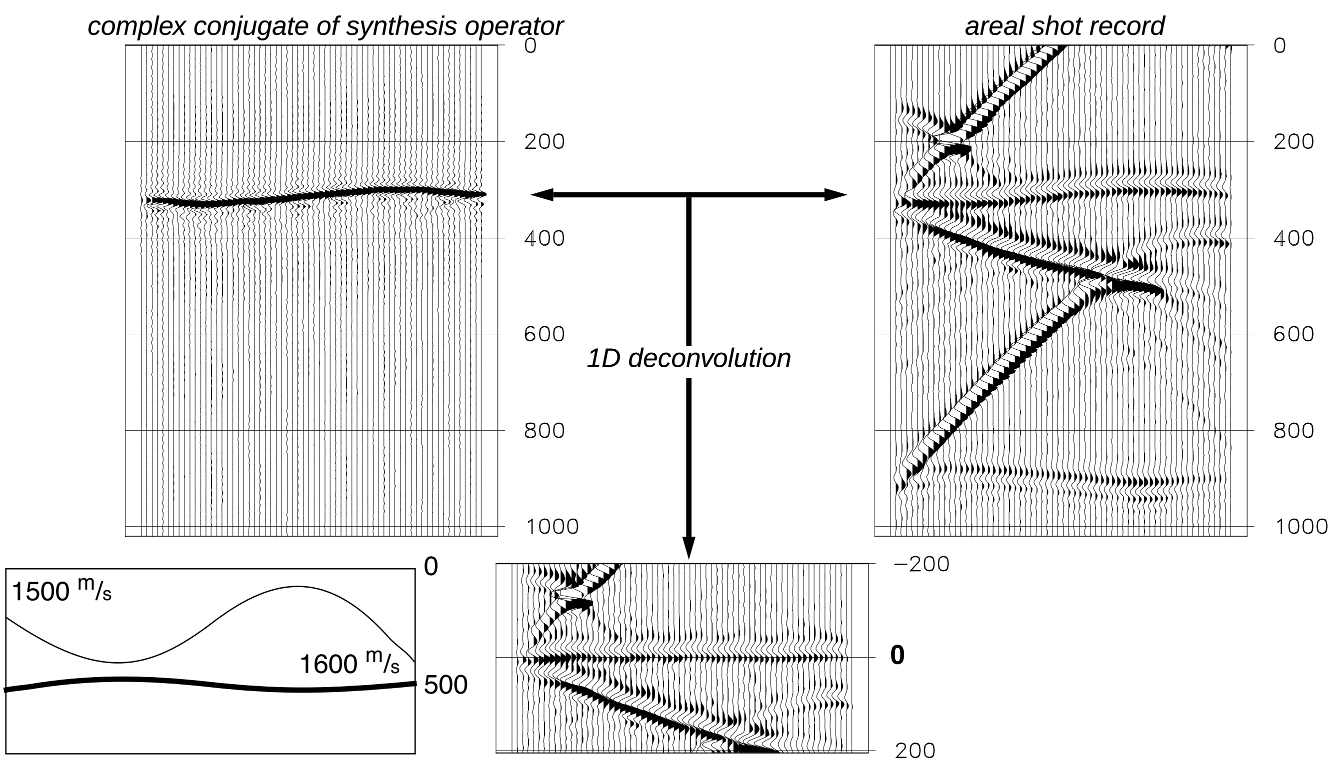

Figure 10.5: *The complex conjugate of the synthesis operator for a* normal incidence *illumination of the second boundary of the model (left), and its areal shot record (right). Note that in the deconvolution display the event does align at* t=0, *although the used macro model is erroneous.*

First we will look at the result after focus point illumination. Figure 10.6 shows the time responses of the complex conjugate of the synthesis operator and the areal shot record. Note that in the deconvolution result the event does align at $t = 0$, although the macro model was erroneous. Hence with a *focus point* illumination we cannot detect this structural error. This is quite obvious, since the focus point illumination defines a *local* illumination.

We will now look at the result for the normal incidence illumination of the (erroneous) macro boundary. Figure 10.7 shows the time responses of the complex conjugate of the synthesis operator and the areal shot record. Note that in the deconvolution result the event does *not* align at $t = 0$, indicating the used macro model was erroneous. Hence with a *normal incidence* illumination we *can* detect the introduced structural error.

We have shown that different types of errors can be detected by different types of illuminating wavefields. Combined velocity/depth errors can be detected only if the considered macro boundary is illuminated by more than one angle. For this we will use the *focus point* illumination. Since the focus point illumination defines a *local* illumination, errors with lateral extent, like structural errors, cannot be detected by this type of illumination. The normal incidence illumination however is very well suited to detect these type of errors, hence to *validate* an entire macro boundary.

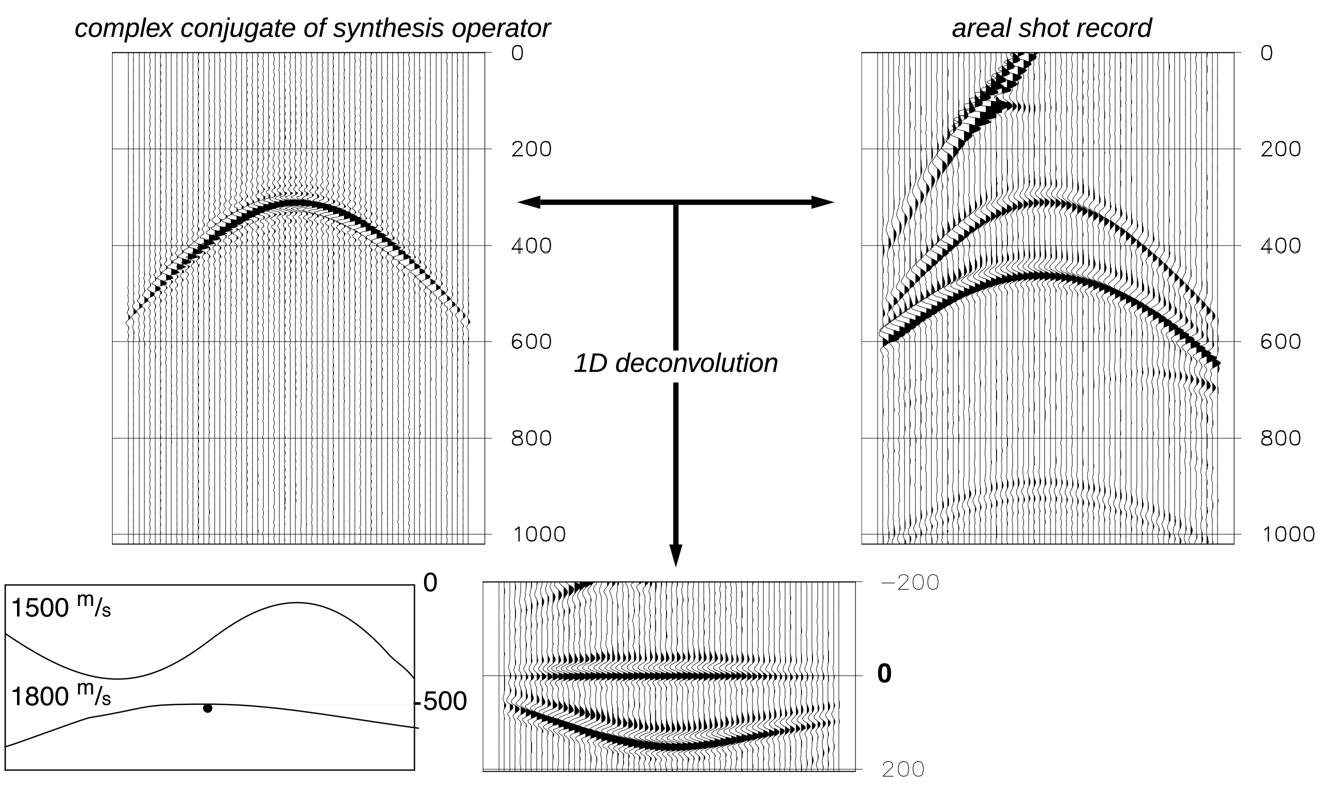

Figure 10.6: *The complex conjugate of the synthesis operator for a* focus point *illumination of the second boundary of the model (left), and its areal shot record (right). Note that in the deconvolution display the event* does *align at* t=0*, although the used macro model is erroneous.*

If we assume that the velocity within a macro boundary does not change rapidly in a lateral sense, we can, after solving the velocity/depth errors using focus point illuminations at several sparse distributed positions along a macro boundary, use the normal incidence illumination to *update* the structure of the macro boundary. The focus point illumination results are in that case used as calibration points. Additional focus point illuminations can be used to evaluate whether the assumption on the lateral velocity changes was valid.

10.4 In quest of updating formulas

Sofar we have seen that we can evaluate macro boundaries, and that we are able to detect different types of errors in the macro model by using different types of illuminating wavefields. In this section we will derive formulas to update the macro model. First we will derive a general formulation of how errors in the macro model will show up in both the synthesis operator and the areal shot record.

10.4.1 General formulation

Let us first recall the forward model for a single reflector and the definition of the synthesis operator:

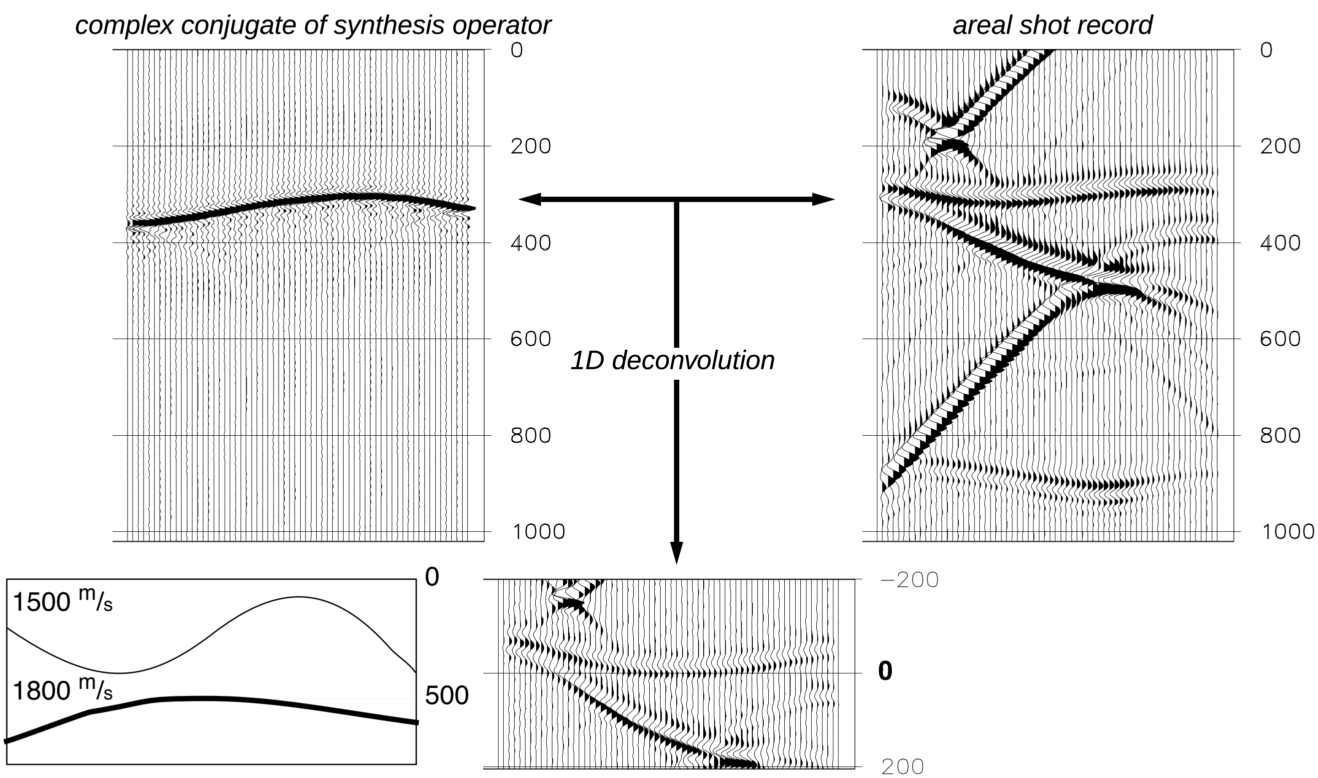

Figure 10.7: *The complex conjugate of the synthesis operator for a* normal incidence *illumination of the second boundary of the model (left), and its areal shot record (right). Note that in the deconvolution display the event does not align at* t=0*, indicating an error in the macro model.*

$$\boldsymbol{P}^{-}(z_0) = \boldsymbol{W}^{-}(z_0,z_m)\, \boldsymbol{R}(z_m)\, \boldsymbol{W}^{+}(z_m,z_0)\, \boldsymbol{S}^{+}(z_0), \tag{10.10a}$$

and

$$\vec{\Gamma}^{+}(z_0) = [\overline{\boldsymbol{W}}^{-}(z_0,z_m)]^{*}\, \vec{\Gamma}^{+}(z_m), \tag{10.10b}$$

where the operators $\boldsymbol{W}^{-}$ and $\boldsymbol{W}^{+}$ describe the propagation properties of the true medium, whereas the $\overline{\boldsymbol{W}}^{-}$ operator describes the propagation properties in the estimated macro model. The complex conjugate of the $\overline{\boldsymbol{W}}^{-}$ operator is the matched filter approximation to the inverse of the $\overline{\boldsymbol{W}}^{+}$ operator in the estimated macro model.

If we assume that we can describe the propagation in the macro model $\overline{\boldsymbol{W}}^{-}(z_0,z_m)$ by the propagation in the true medium $\boldsymbol{W}^{-}(z_0,z_m)$, and a correction term $\Delta\boldsymbol{W}(z_m)$, we can rewrite equation (10.10b) as:

$$\vec{\Gamma}^{+}(z_0) = [\boldsymbol{W}^{-}(z_0,z_m)\, \Delta\boldsymbol{W}(z_m)]^{*}\, \vec{\Gamma}^{+}(z_m). \tag{10.11}$$

Application of the synthesis operator $\vec{\Gamma}^{+}(z_0)$ to the data, using equation (10.2) and taking a unit source signature S(ω), leaves the areal shot record $\vec{P}^{-}_{syn}(z_0)$ as:

$$\vec{P}^{-}_{syn}(z_0) = \boldsymbol{W}^{-}(z_0,z_m)\, \boldsymbol{R}^{+}(z_m)\, [\Delta\boldsymbol{W}(z_m)]^{*}\, \vec{\Gamma}^{+}(z_m). \tag{10.12a}$$

Using a first order approximation for $\Delta\boldsymbol{W}(z_m)$ (Berkhout, 1985) and using a diagonal assumption for the reflectivity matrix $\boldsymbol{R}^{+}(z_m)$, equation (10.12a) simplifies to:

$$\vec{P}^{-}_{syn}(z_0) \approx \boldsymbol{W}^{-}(z_0,z_m)\, [\Delta\boldsymbol{W}(z_m)]^{*}\, \boldsymbol{R}^{+}(z_m)\, \vec{\Gamma}^{+}(z_m), \tag{10.12b}$$

or

$$\vec{P}^{-}_{syn}(z_0) \approx \boldsymbol{W}^{-}(z_0,z_m)\, [\Delta\boldsymbol{W}(z_m)]^{*}\, \vec{R}^{+}(z_m). \tag{10.12c}$$

The first order approximation of $\Delta\boldsymbol{W}(z_m)$ means that we allow one traveltime correction per lateral position, hence $\Delta\boldsymbol{W}(z_m)$ becomes a *diagonal* matrix. Using a diagonal assumption for the reflectivity matrix $\boldsymbol{R}^{+}(z_m)$ means that we only use the *zero-offset* reflectivity of the macro boundary. This simplification is allowed since in macro model estimation the main interest is a good match of the traveltimes and not for the amplitudes.

Updating formulas should be based on the relation between the areal shot record $\vec{P}^{-}_{syn}(z_0)$, as described by equation (10.12c), and the complex conjugate of the synthesis operator $\vec{\Gamma}^{+}(z_0)$:

$$[\vec{\Gamma}^{+}(z_0)]^{*} = \boldsymbol{W}^{-}(z_0,z_m)\, \Delta\boldsymbol{W}(z_m)\, [\vec{\Gamma}^{+}(z_m)]^{*}. \tag{10.12d}$$

In the next subsections we will present the updating formulas based on the given general formulation. The updating formulas will be derived on bases of traveltime curves in both the synthesis operator and the areal shot record.

10.4.2 Searching for updating formulas for a flat reflector

Assuming a flat reflector in the subsurface we will derive analytical expressions for the curves observed in the synthesized shot record. We will regard only the arrival times of the reflections and do not take the amplitude variations into account. The well known traveltime curve for a flat reflector at depth z with a source at position x_s and a receiver at x_d is described by

$$T_d(x_d, x_s) = \frac{\sqrt{4z^2 + (x_d - x_s)^2}}{c}, \tag{10.13}$$

where the subscript d in T_d refers to the data and c is the velocity of the medium above the reflector. The traveltime curve for a synthesis operator with a focussing point at $(0, z + dz)$ in the subsurface is given by

$$\bar{T}_s(x_s) = \frac{\sqrt{(z + dz)^2 + x_s^2}}{c + dc}, \tag{10.14}$$

where the subscript s in T_s refers to the synthesis operator (see also Figure 10.8) and dz and dc represent the depth and velocity error with respect to the true model. The bar above T_s denotes to an estimation of the true model.

Application of the synthesis operator to a common detector gather (fixed x_d) can be interpreted as a time convolution between the traces of the data and the conjugate of the traces of the synthesis operator. In terms of traveltimes this time convolution is represented by

$$T_d(x_d, x_s) - \bar{T}_s(x_s) = \frac{\sqrt{4z^2 + (x_d - x_s)^2}}{c} - \frac{\sqrt{(z + dz)^2 + x_s^2}}{c + dc}. \tag{10.15}$$

From the two-way traveltime from source to reflector and back to receiver, one way, from source to reflector, is peeled off by the synthesis operator. The synthesis process itself is a summation over all the convolved traces of the 'synthesized' common detector gather so,

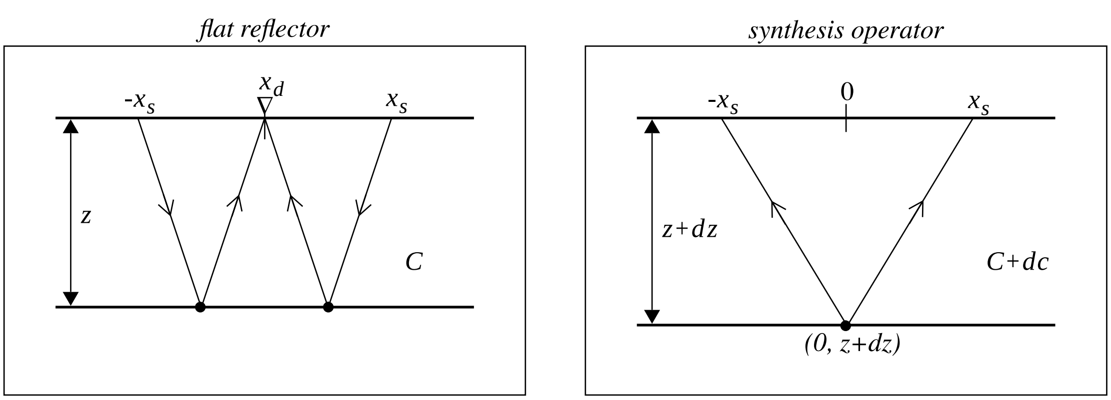

Figure 10.8: *Ray paths for a flat reflector (left) and a point focussed synthesis operator (right).*

$$\vec{P}^{-}_{syn}(x_d) = \sum_{x_s} A(x_d, x_s)\, exp\,(j\omega(T_d(x_d, x_s) - \overline{T}_s(x_s))) \tag{10.16}$$

where A is an amplitude factor. Equation (10.16) gives the synthesized trace, in the frequency domain, for one common detector position. Repeating the process for all common detector positions will give the synthesized shot record. Equation (10.16) is the discrete version of the integral

$$\vec{P}^{-}_{syn}(x_d) = \int_{x_s} A(x_d, x_s)\, \exp\,(j\omega\phi(x_d, x_s))\, dx_s, \tag{10.17}$$

where $\phi(x_d, x_s)$ represents the traveltime function. Equation (10.17) is a well known integral which solution can be approximated by using the stationary phase method. The stationary phase approximation simplifies the summation in Equation (10.16) to the evaluation of the stationary points with respect to x_s. The stationary points of Equation (10.15) are given by

$$\frac{\partial}{\partial x_s}(T_d - \overline{T}_s) = 0, \tag{10.18}$$

$$= \left(\frac{(x_s - x_d)}{c\sqrt{4z^2 + (x_s - x_d)^2}} - \frac{x_s}{(c + dc)\sqrt{(z + dz)^2 + x_s^2}}\right) \tag{10.19}$$

which solution is equivalent to

$$(x_s - x_d)\,(c + dc)\sqrt{(z + dz)^2 + x_s^2} - x_s c\sqrt{4z^2 + (x_s - x_d)^2} = 0. \tag{10.20}$$

Solving Equation (10.20) for x_s in a closed form is not trivial, but by considering only a depth or velocity error we can derive, by inspection and numerical evaluation, some properties of the stationary point and the synthesized shot record. Having found the stationary point we replace the summation in Equation (10.16) by the evaluation of the stationary point into the phase and do this for all common detector gathers to find the traveltime curve for the synthesized shot record.

Zero depth and zero velocity error ($dz=0$ and $dc=0$)

Using the correct macro model will give for the synthesized shot record exactly the same hyperbola as the synthesis operator. Equation (10.20) reduces then to

$$(x_s - x_d)\, c\sqrt{z^2 + x_s^2} - x_s c\sqrt{4z^2 + (x_s - x_d)^2} = 0 \tag{10.21}$$

which has the simple solution $x_s = -x_d$. Substituting this solution (stationary point) in Equation (10.15) for all common detector positions gives for the synthesized shot record

$$T_d(x_d, -x_d) - \overline{T}_s(-x_d) = T_{syn}(x_d) = \frac{\sqrt{z^2 + x_d^2}}{c}, \tag{10.22}$$

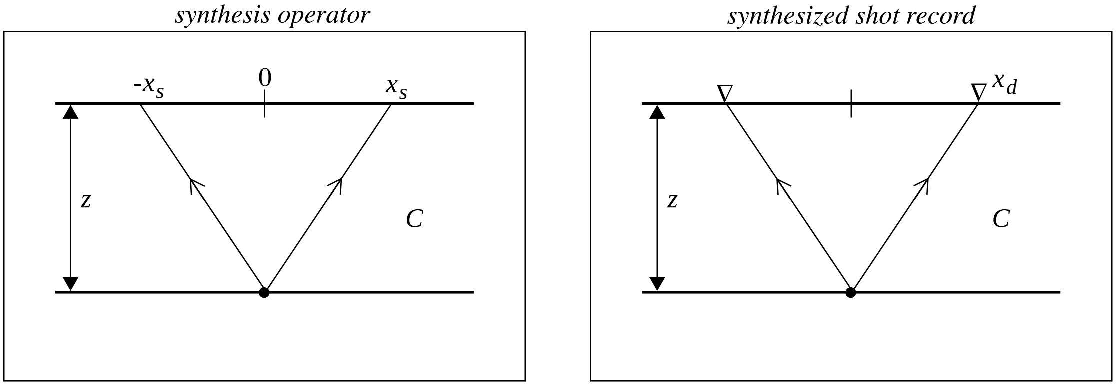

Figure 10.9: *Ray paths for the synthesis operator (left) and the synthesized shot record(right) using the correct macro model.Note that the figures are the same.*

with the synthesis operator

$$\bar{T}_s(x_s) = \frac{\sqrt{z^2 + x_s^2}}{c}. \tag{10.23}$$

Note that Equation (10.23) is indeed the same as Equation (10.22). In Figure 10.8 some ray paths are given for the synthesis operator and the synthesized shot record using the correct macro model.

Depth errors (dz=±dz and dc=0)

In the case of a positive depth error and a zero velocity error Equation (10.20) reduces to

$$(x_s - x_d)c\sqrt{(z + dz)^2 + x_s^2} - x_s c\sqrt{4z^2 + (x_s - x_d)^2} = 0 \tag{10.24}$$

The solution for the stationary points in this equation can still be expressed in a closed form (with the aid of Mathematica on a NeXT computer) and is given by

$$x_s = x_d \frac{(dz + z)}{(dz - z)}. \tag{10.25}$$

Substitution of this solution in Equation (10.15) gives for the synthesized shot record

$$T_{syn}(x_d) = \frac{\sqrt{(z - dz)^2 + x_d^2}}{c}. \tag{10.26}$$

The synthesis operator is given by

$$\bar{T}_s(x_s) = \frac{\sqrt{(z + dz)^2 + x_s^2}}{c}. \tag{10.27}$$

From Equation (10.27) is it observed that the time correction, to the down going source wave field at the surface, with the synthesis operator is for a positive dz too large. The synthesized

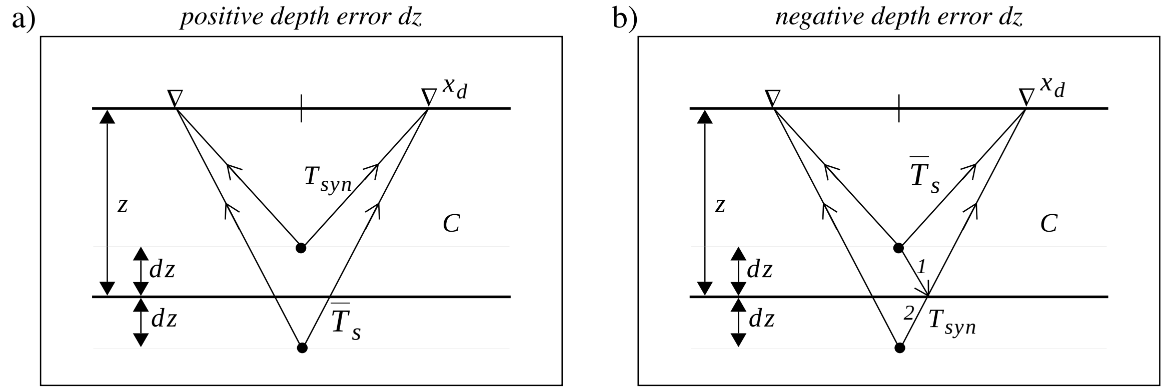

Figure 10.10:*Depth errors in the synthesis operator (T_s): depth too deep (a) and depth too shallow (b) gives different synthesized shot records (T_{syn}), which can be interpreted as the response of a virtual source above or below the reflector.*

shot record can therefore be interpreted as the response of a virtual source above the reflector (see Figure 10.10a).

For a negative dz the time correction with the synthesis operator is too small and the synthesized shot record can be interpreted as the response of a virtual source below the reflector position (or alternatively as the reflected response from a source above the reflector, see Figure 10.10b).

Velocity errors (dz=0 and dc=±dc)

If there is only a velocity error in the synthesis operator Equation (10.20) reduces to

$$(x_s - x_d)\ (c + dc)\sqrt{z^2 + x_s^2} - x_s c\sqrt{4z^2 + (x_s - x_d)^2} = 0. \tag{10.28}$$

Unfortunately it is not possible too find a closed form solution for this equation. We therefore have solved Equation (10.28) numerically for a set of different parameters. Based on these numerical results we have observed the following:

If the velocity error dc is negative, thus using a velocity in the calculation of the synthesis operator which is too low there is always one real numerical solution of Equation (10.28). This means that there is at least one stationary point which gives a contribution to the summation of Equation (10.16). This single contribution will lead to a simple picture for the synthesized shot record.

If the velocity error dc is positive, thus using a velocity in the calculation of the synthesis operator which is too large, there are always at least two real numerical solutions found. This means that there are two stationary points which both give a contribution to the summation of Equation (10.16). This may lead to a more complicated picture for the synthesized shot record. The numerical experiments also showed that one of the two stationary points found lays far from x_s=*0*.

Common detector gathers prior to synthesis

A picked time section out of the common detector gather prior to synthesis, thus before summation over all traces, can also give more insight in the shape of the synthesized shot record. This picked time section, for different parameters, can be calculated by using Equation (10.15). We use a simple model with only one reflector 300 m. below the source and receiver positions. The receivers in this model are positioned from -1770 m. to 1770 m. with a spatial interval of 15 m. The 237 shots are positioned at all detectors positions from the first detector position at -1770 m to the last detector position at 1770 m. with a spatial interval of 15 m.

In Figure 10.11 four different time sections are shown for depth and velocity errors as function of the detector position in the model for three different common detector positions. The common detector sections for $x_d = 0$ show for the depth errors only one stationary point at $x_s = 0$. The other common detector positions ($x_d = 450$ and $x_d = 900$) have a shifted stationary point position which position on the x_s-as is given by Equation (10.25). The time sections with a velocity which is smaller than the true velocity show that there exists indeed one stationary point, although we could not (yet) derive it. For a velocity higher than the true velocity we cannot observe any stationary point for the common detector positions at $x_d = 450$ and $x_d = 900$ and it is not possible to forecast, with the aid of the time section, how the synthesized shot

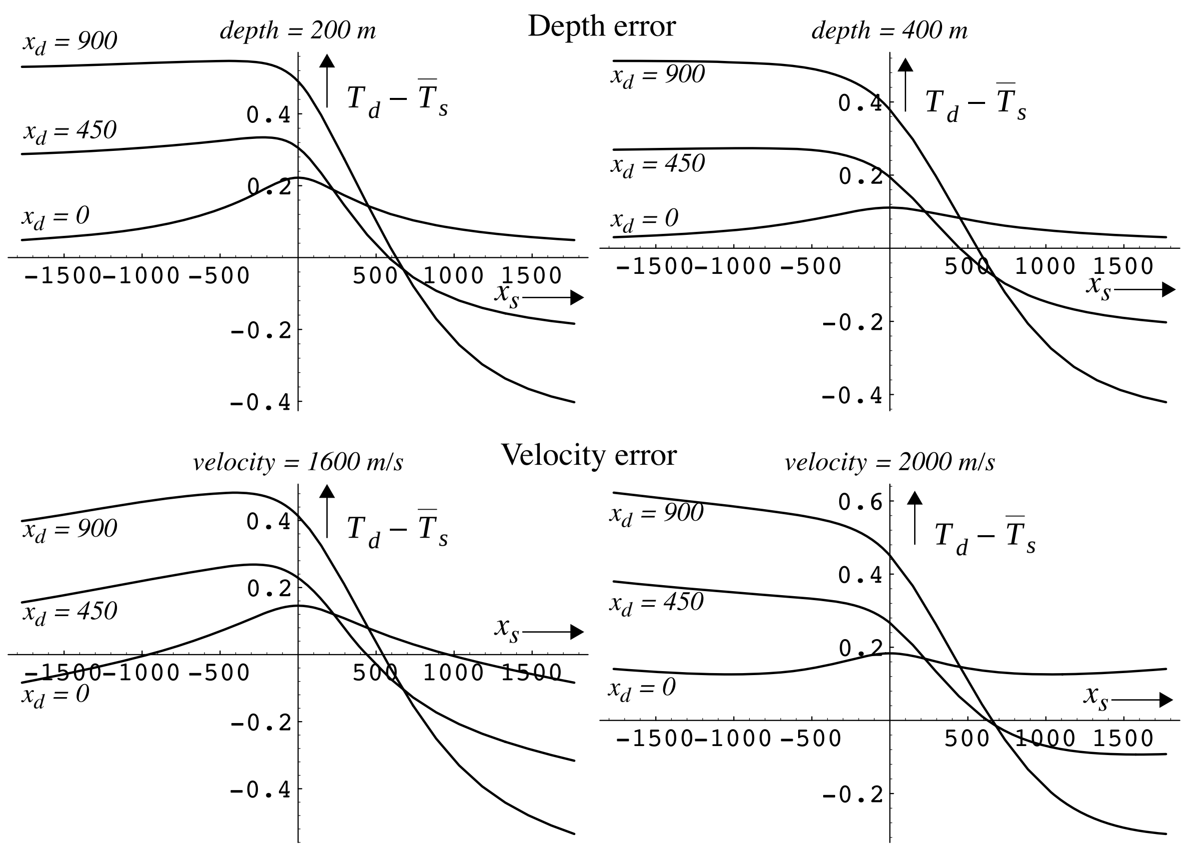

Figure 10.11:*Time sections of the common detector gathers prior to synthesis as function of the detector position for different depth and velocity errors in the synthesis operator. For the velocity error of 2000 m/s the contribution to the summation in equation (10.16) will be more complex due to the lack of stationary points.*

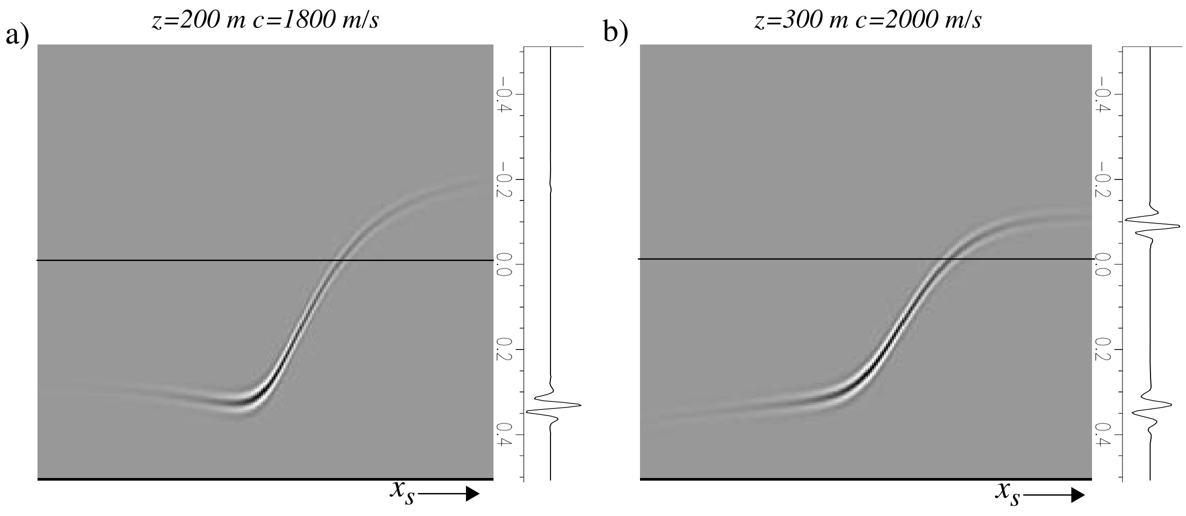

Figure 10.12: *a) Common detector gather with a depth error of -100 m in the synthesis operator.*
b) Common detector gather with a velocity error of +200 m/s in the synthesis operator.
Note the double contribution of the gather with a positive velocity error.

record will look like. It is therefore also not possible to derive a closed form for the updating formula's, which is what we are looking for.

Instead of using Equation (10.15) to calculate the time sections for the common detector gathers prior to synthesis we can convolve the common detector gather under consideration with the conjugate of the synthesis operator to obtain the same results. The resulting record is shown in Figure 10.12a for a common receiver gather at position x_d = 450 and a depth error in the synthesis operator of -100 m (depth = 200 m). In Figure 10.12b the same common receiver gather is shown with a synthesis operator with a velocity error of +200 m/s (velocity = 2000 m/s). In both pictures the same shape of the time section as in Figure 10.11 can be observed. The result of the summation over all traces is also given in Figure 10.12. The summation shows that the position of the stationary point in Figure 10.12a is indeed the only contribution in the summation. However, in Figure 10.12b we see two contributions in the synthesized trace.

Synthesized shot records deconvolved with the synthesis operator

The summation over all the receivers in a common receiver gather is done for all common detector gathers to arrive at the synthesized shot record. If the correct macro model is used it has been shown that this synthesized shot record contains exactly the same event as the synthesis operator. But what if there is an error in the macro model? A time deconvolution of the synthesized shot record with the synthesis operator gives

$$T_{dec}(x_d) = T_{syn}(x_d) - \overline{T}_s(x_s{=}x_d) \qquad (10.29)$$

which represents the time difference between the two records. This time difference can be used to find an update. If we know the exact traveltime curve for T_{dec}, which is dependent on the errors made, then it is possible to compare these analytical curves (in a least squares way) with

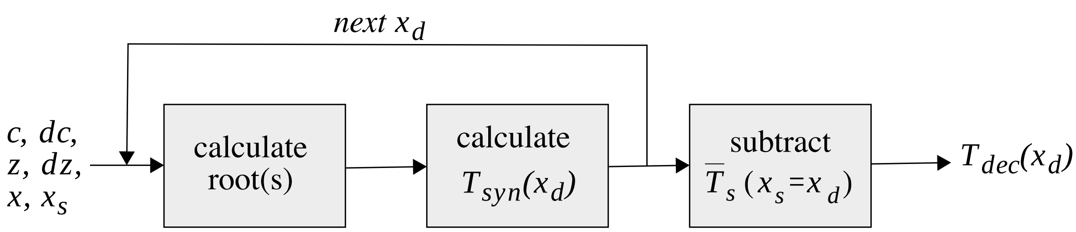

Figure 10.13:*Numerically calculation of T_{dec} for a common detector gather with a velocity and depth error.*

the observed curve. It has been shown that for a depth error in the macro model it is possible to derive a closed form expression for T_{dec}. In this ideal case only one update is sufficient to arrive at the correct answer. For a velocity, or a depth and velocity, error we could not derive such a closed form. In that case we have to use numerical methods to calculate the stationary points in Equation (10.15) in order to determine T_{dec}. For practical situations we will always solve Equation (10.20) numerically. The scheme given in Figure 10.13 calculates T_{dec} in a numerical way such that it can be used in an updating scheme. The calculation of the roots of Equation (10.20) is done with a Newton-Raphson method (Press, Numerical Recipes in C, 1992). For negative velocity errors and negative and positive depth errors there is only one root and the method can be used straight forward. For positive velocity errors a-priori knowledge of the position of the roots has to be built in the algorithm (which will be done in the near future). At the moment we will not consider these positive velocity errors and focus our attention on the convergence of the proposed updating scheme.

In Figure 10.14 the deconvolved results are shown for different velocity and depth errors in the macro model used in the synthesis calculation. The same model as described in section is used again to arrive at the results shown in Figure 10.14. If the correct model is used the deconvolved result shows an event which aligns at zero time. For a negative velocity error the deconvolved records contain one simple event (originating from the single stationary point). But positive velocity errors in the synthesis operator results in a complicated deconvolved event (originating from the multiple stationary points). The positive and negative depth errors are symmetric with respect to the zero time lag in the deconvolved sections and contain only one single event. At the bottom of Figure 10.14 the numerically calculated curves are shown for the different velocity and depth errors. The curves for the depth errors are calculated correctly for both positive and negative depth errors. The curves for the velocity errors are only correct for the negative velocity errors, the positive velocity errors show the contribution of one stationary point only.

In Figure 10.15 the deconvolved synthesized shot record for both a depth and velocity error in the macro model are shown for different combinations of depth and velocity errors. For a positive velocity error the complicated deconvolved results show up again. The negative velocity errors together with a positive or negative depth error are used to test the scheme proposed in Figure 10.13.

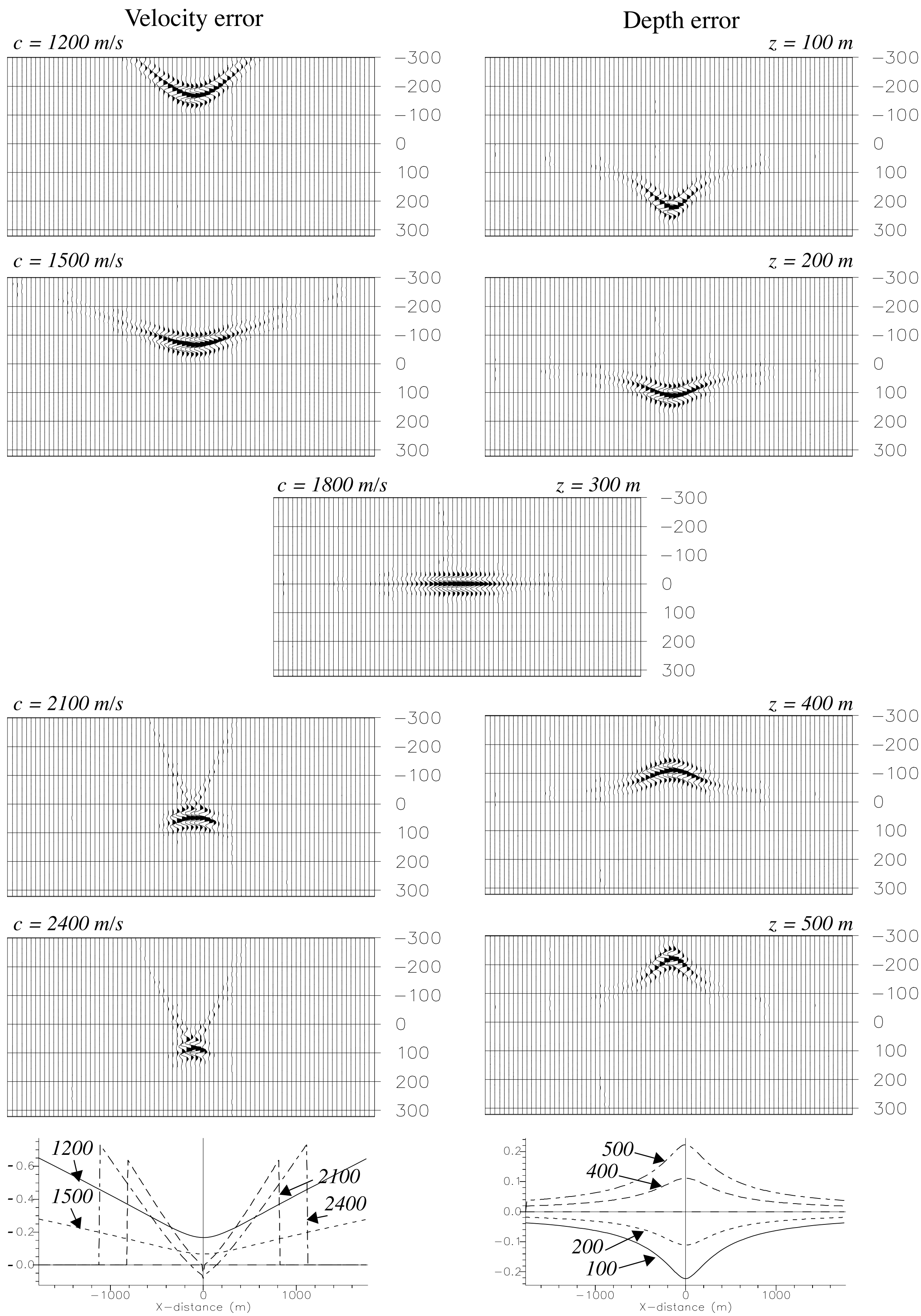

__Figure 10.14:__ Deconvolution of the synthesized shot record with its synthesis operator for different velocity and depth errors in the synthesis operator. Numerically calculated curves are shown below. These curves predict the behavior of the deconvolved synthesized shot record correctly, except for the positive velocity errors.

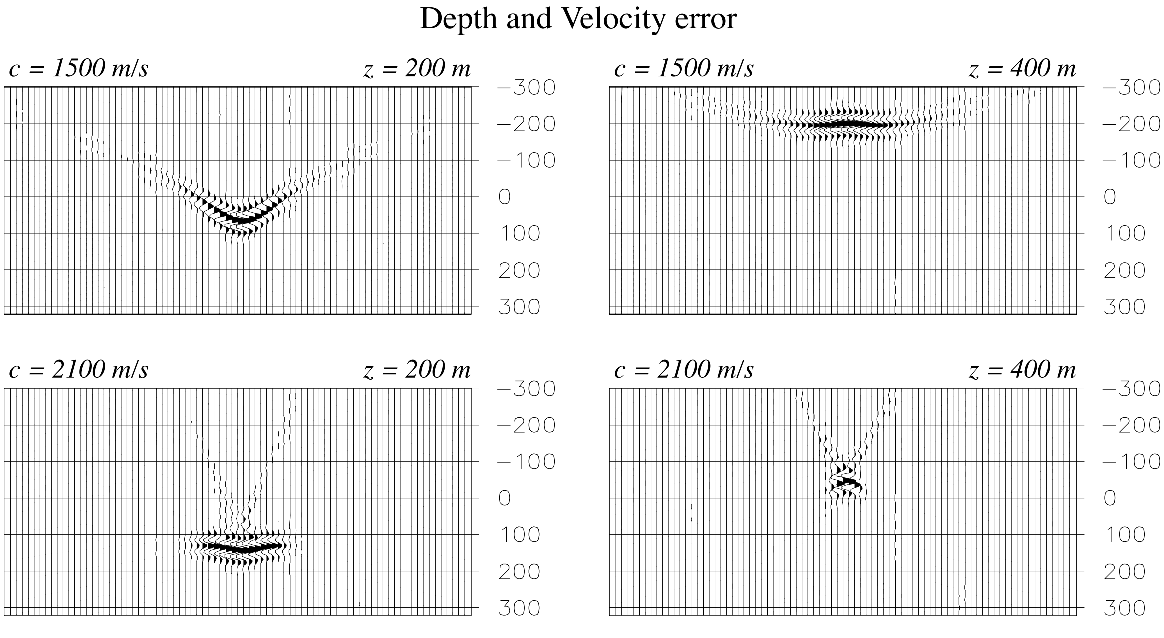

Figure 10.15: *Synthesized shot record deconvolved with its synthesis operator for different velocity and depth errors. Note that for negative velocity errors simple curves are observed.*

After numerical calculation of T_{dec} this calculated curve is compared in a least squares manner with the tracked time section of Figure 10.15. The domain, in which the search for a match with the tracked section is carried out, is in depth varying from 100 to 500 m with steps of 5m and in velocity from 1500 to 2100 m/s with steps of 10 m/s. So in this domain the numerical calculation for T_{dec} is done. The tracked time sections of the two synthesized shot records in Figure 10.15 with the negative velocity error are the curves to be matched. The results are shown in Table 10.1 for the five best matches. Note, that the estimated depth and velocity update gives directly the correct answer so calculation of another synthesis operators is not needed in this case. In Table 10.1 it can be seen that the best match, based on the least squares criterion, can

Table 10.1: *The five best matches for the time section out of Figure 10.15 for the negative velocity errors left for the negative depth error and right for the positive depth error. The best match can be distinguished clearly from the other nearest matches.*

velocity(m/s)	**depth(m)**	**least-squares fit**	**velocity(m/s)**	**depth(m)**	**least-squares fit**
1800	300	0.000326	1800	300	0.000288
1810	305	0.001940	1800	305	0.002404
1800	305	0.003001	1810	305	0.003013
1810	300	0.004144	1810	310	0.004327
1810	310	0.004872	1810	315	0.009846

be distinguished clearly from the other four nearest matches. The best match together with the

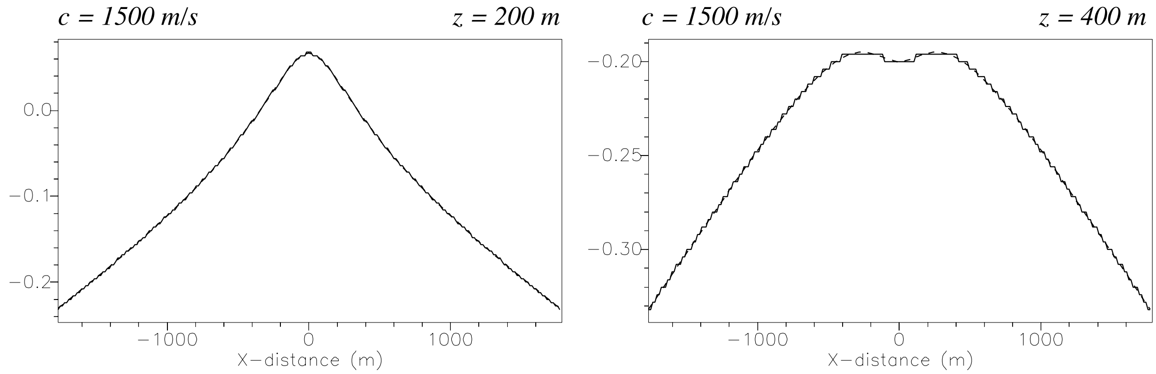

Figure 10.16:*Best match for the tracked time section of Figure 10.15 (dotted line represents the match). Note the perfect match of the tracked curve with the calculated curve.*

tracked time section are shown in Figure 10.16. Note the perfect match between the tracked time section and the calculated curve.

We have shown that it is possible to calculate analytical curves for the different depth and velocity errors. By comparing the tracked time section of the, for the synthesis operator deconvolved, synthesized shot record with the calculated curves it is possible to correct the initial estimate. With this correction a new macro model can be built and a new correction can be found. This recursive technique will terminate when the deconvolved synthesized shot record has a straight event at zero time. In that case the synthesis operator and the event under consideration in the synthesized shot record are exactly the same. The diagram of this recursive estimation technique is given in Figure 10.17.

10.5 Conclusions and Future plans

A *focus point* illumination can detect depth/velocity errors in the macro model at calibration points. The *normal incidence* illumination can be used to validate the interpolation results between the calibration points.

Using a focussing synthesis operator derived from an initial macro model there are in general three unknowns: the velocity of the medium, and the depth of the reflector. To find an update for an initial guess, analytically calculated curves can be used to find the best fit with the tracked crosscorrelation. In the ideal case only one iteration is needed to arrive at the correct model. But due to tracking errors in difficult media there are in general more iterations needed. In the near future we will investigate the use of a non linear least squares optimization algorithm. We will also aim at a closed form expression for the updating formulas in the case of a positive velocity error and dipping reflectors by numerical analysis and inspection of the equations of interest. The method is very well suitable for 3D-irregular datasets.

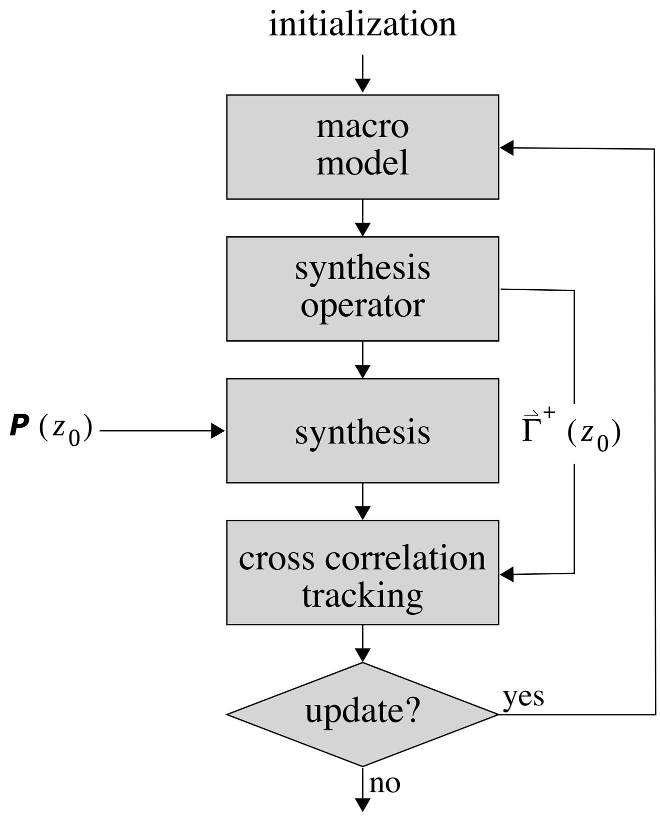

Figure 10.17:*Proposed updating procedure for macro model estimation*

10.6 References

Berkhout, A.J., 1985, *Seismic migration: Imaging of acoustic energy by wave field extrapolation. A. Theoretical Aspects*. 3rd Edition: Elsevier Science Publ. Co., Inc.

DELPHI, 1992, Volume III, Chapter 5, *Macro shot record technology*, 149 - 162, Delft University of Technology.

DELPHI, 1993, Volume IV, Chapter 10, *Macro model estimation by means of controlled illumination*, 233 - 250, Delft University of Technology.

Press, W.H., Teukolsky, S.A., Vetterling, W.T. and Flannery, B.P., 1992, *Numerical Recipes in C, The Art of Scientific Computing*, Second Edition, Cambridge University Press.

Wapenaar, C.P.A. and Berkhout, A.J., 1989, *Elastic wave field extrapolation, Redatuming of single-and multi-component seismic data*: Elsevier Science Publishers.